Advances in Materials Research, *Vol. 13, No. 1 (2024) 37-53*
https://doi.org/10.12989/amr.2024.13.1.037

Interfacial stresses in porous PFGM-RC hybrid beam

Benferhat Rabia[1,2], Hassaine Daouadji Tahar*[1,2] and Rabahi Abderezak[1,2]

[1]*Civil Engineering Department, University of Tiaret, Algeria*
[2]*Laboratory of Geomatics and Sustainable Development, University of Tiaret, Algeria*

(*Received September 3, 2021, Revised May 10, 2023, Accepted July 11, 2023*)

Abstract. This paper presents a careful theoretical investigation into interfacial stresses in RC beams strengthened with externally bonded imperfect FGM plate. In this study, an original model is presented to predict and to determine the stresses concentration at the imperfect FGM end, with the new theory analysis approach. Stress distributions, depending on an inhomogeneity constant, were calculated and presented in forms. It is shown that both the shear and normal stresses at the interface are influenced by the material and geometry parameters of the composite beam, and it is shown that the inhomogeneities play an important role in the distribution of interfacial stresses. The theoretical predictions are compared with other existing solutions. The numerical resolution was finalized by taking into account the physical and geometric properties of materials that may play an important role in reducing the stress values. This research is helpful for the understanding on mechanical behaviour of the interface and design of the PFGM-RC hybrid structures.

Keywords: imperfect FGM plate; interfacial stresses; porosity; RC beam; strengthening

1. Introduction

The major problem encountered in the field of construction in the world concerns the aging of civil engineering structures which are built according to methods classic and old. In Algeria, more than 70% of the works are over 50 years old, especially bridges, which require modernization and rehabilitation works to meet current standards and needs. This research is one of the methods of reinforcement and repair using composite materials type imperfect FGM. It is considered as an effective solution to deal with certain phenomena, such as artificial degradation, corrosion, charge assignments, the earthquakes. The purpose of our work is to determine the interfacial stresses of structures subjected to loads mechanical taking into account shear lag model (Tounsi 2009, Shen 2001). In particular, reliable evaluation of the adhesive shear stress and of the stress in the CFRP plates is mandatory in order to predict the beam's failure load. Recently, the authors conducted a numerical study on the static behaviour of RC beams strengthened with composites in different directions (Smith 2001, Hassaine Daouadji 2013, Hassaine Daouadji *et al.* 2019, Benferhat *et al.* 2021, Tlidji *et al.* 2021a, Sahmani *et al.* 2020, Jena *et al.* 2021, Thanh *et al.* 2022, Adim *et al.* 2016b, Belkacem *et al.* 2016,Rostami *et al.* 2022, Changlin *et al.* 2020, Khaniki *et al.* 2022, Bensattalah *et al.* 2020, Bensattalah *et al.* 2018,Masayuki *et al.* 2020, Pegah *et al.* 2020, Ebrahimi *et al.* 2022,

*Corresponding author, Professor, E-mail: daouadjitahar@gmail.com

http://www.techno-press.org/?journal=amr&subpage=5 ISSN: 2234-0912 (Print), 2234-179X (Online)

Benferhat *et al.* 2019, Abdelhak *et al.* 2021, Kablia *et al.* 2020, Bekkaye *et al.* 2020, Bourada *et al.* 2020, Wattanasakulpong *et al.* 2014, Yüksel *et al.* 2021). Numerical examples and a parametric study are presented to illustrate the governing parameters that control the stress concentrations at the edge of the imperfect FGM strip. Finally, the results of these investigations show that the interface bond-stresses are non-uniformly distributed along the reinforced boundaries. It is believed that the present results will be of interest to civil and structural engineers and researchers (Hassaine Daouadji *et al.* 2022, Benferhat *et al.* 2018, Rabia *et al.* 2019, Rabahi *et al.* 2021b, Hassaine Daouadji *et al.* 2021a).

Our originality consists in improving the works (Kaddari *et al.* 2020, Laib Salaheddine *et al.* 2021, Muhammad Safeer, *et al.* 2021, Adim *et al.* 2016a, Hassaine Daouadji 2017, Hassaine Daouadji *et al.* 2016a, Rabahi *et al.* 2023, Rabahi *et al.* 2022a, Bensatallah *et al.* 2021, Tlidji *et al.* 2021b, Taj Muhammad *et al.* 2021) done previously in order to determine the amplitude of the interfacial stresses of the beams reinforced by the imperfect FGM (Wattanasakulpong 2014, Mehdi *et al.* 2020, Seyed *et al.* 2020a, Amirmahmoud *et al.* 2020, Rabahi *et al.* 2022b, Rabahi *et al.* 2021a, Behrouz *et al.* 2020, Babak *et al.* 2020, Ebrahimi *et al.* 2020, Hua *et al.* 2020, Gui-Lin *et al.* 2020, Raad *et al.* 2020, Seyed *et al.* 2020b, Ridha *et al.* 2020, Hassaine Daouadji *et al.* 2021d, Hassaine Daouadji *et al.* 2021e, Benferhat *et al.* 2021c, Benferhat *et al.* 2020, Kablia *et al.* 20022, Bo Yu *et al.* 2021, Guenaneche *et al.* 2019) reinforcements while taking into account neglected parameters, in particular, the shear deformations of the beam and the plate and the effect the porosity of the reinforcement plate (as manufacturing defect) which have a great influence on the value of the stress concentration and on the delaminating phenomenon. The choice of the shapes of the elements of the structure and the composite materials makes it possible to reduce the amplitude of these interfacial constraints. However, our work improves the numerical resolution of normal and shear stresses and can also adapt to all types of structures having different shapes and different materials. The present study concerns the shear and normal stresses concentrations at the ends of the imperfect FGM plate (Hassaine Daouadji *et al.* 2016b and Rabia *et al.* 2016). In this paper, the details of the interfacial stress are analyzed by the improved theoretical solutions. The effects of the material and geometry parameters on the interface stresses are considered and compared with that resulting from literature.

2. Interface stress analysis

2.1 Assumptions

The present analysis takes into consideration the transverse shear stress and strain in the beam and the plate but ignores the transverse normal stress in them. One of the analytical approach proposed by Benferhat (2021a) for reinforced concrete beam strengthened with a bonded imperfect FGM plate (Fig. 1) was used in order to compare it with another analytical models. The theory used in this new approach can be applied to structures of different sections and for different types of materials, taking into account the following appropriate assumptions:

• Elastic stress strain relationship for concrete, imperfect FGM plate and adhesive;
• There is a perfect bond between the FGM plate and the beam;
• The adhesive is assumed to only play a role in transferring the stresses from the concrete to the composite plate reinforcement;
• The stresses in the adhesive layer do not change through the direction of the thickness.

Failure modes at the interface of imperfect FGM reinforced structures are peel and shear stresses

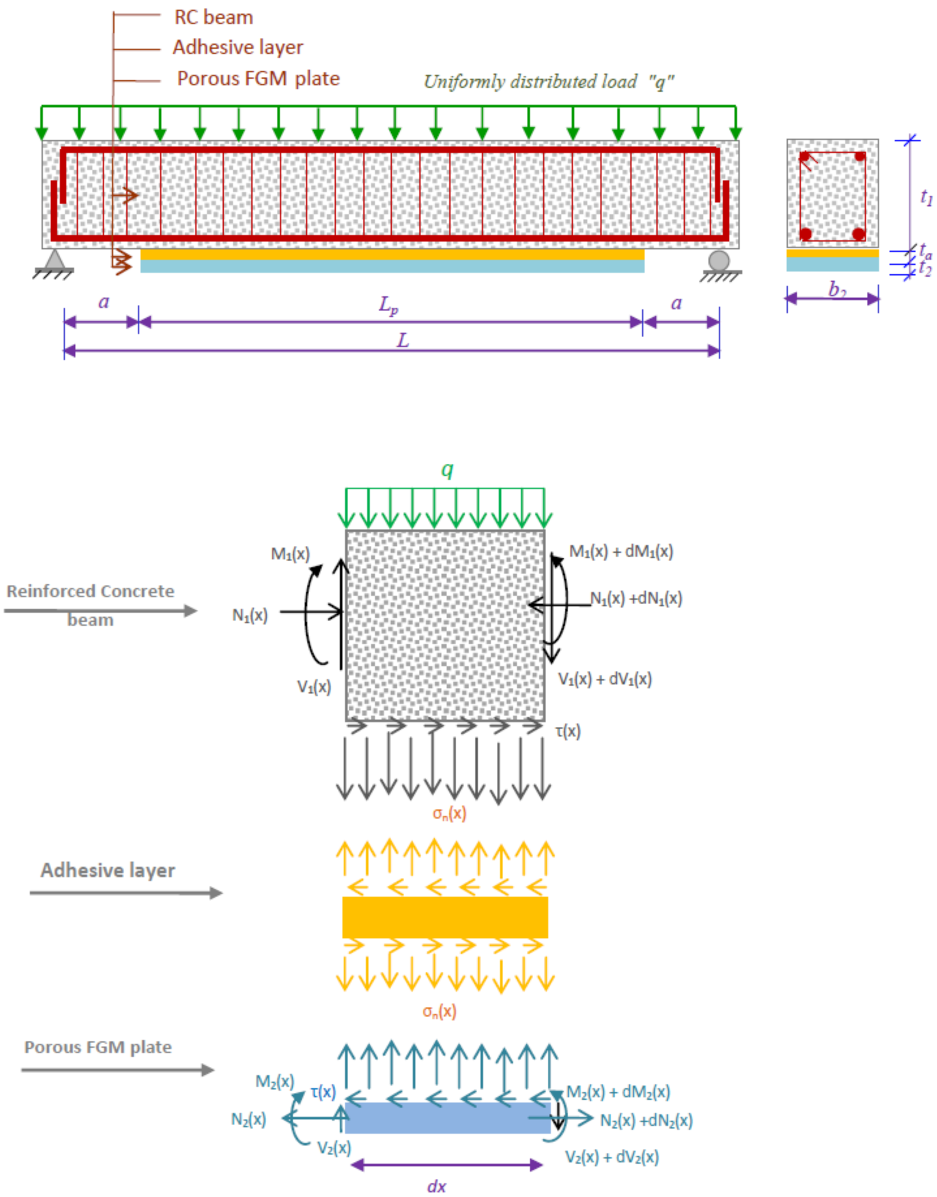

Fig. 1 Simply supported beam strengthened bonded with imperfect FGM plate

at the adhesive joint. They can significantly reduce the strength and rigidity of the structure. Fig. 1 illustrates the shape and geometry of the structure, and shows an infinitesimal element of the structure with applied loads. Since the functionally graded materials is an orthotropic material. In analytical study, the classical plate theory is used to determine the stress and strain behaviours of the externally bonded composite plate in order to investigate the whole mechanical performance of the FGM-strengthened structure (Hassaine Daouadji *et al.* 2021b, Rabia *et al.* 2020, Rabahi *et al.* 2021c).

2.2 Properties of the FGM constituent materials

The FGM can be defined by the variation in the volume fractions. Most researchers use the power-law function or exponential function to describe the volume fractions. Consider an elastic FGM plate of uniform thickness h, which is made of a ceramic and metal, is considered in this study. The material properties, young's modulus and the Poisson's ratio, on the upper and lower surfaces are different but are preassigned according to the performance demands (Benferhat 2021a). However, the Young's modulus and the Poisson's ratio of the plates vary continuously only in the thickness direction (z-axis) i.e., $E=E(z)$, $\nu=\nu(z)$. Thus, Poisson's ratio of the plate is assumed to be constant. However, the Young's modules in the thickness direction of the FGM plates vary with power-law functions (P-FGM). The material properties of P-FGM plates are assumed to vary continuously through the thickness.

$$P = P_m(V_m - \frac{\alpha}{2}) + P_c((\frac{z}{h} + \frac{1}{2})^k - \frac{\alpha}{2}) \tag{1}$$

Where, k is the power law index that takes values greater than or equals to zero. The FGM plate becomes a fully ceramic plate when k is set to zero and fully metal for large value of k. where e_m is the Young's modulus of the homogeneous plate; e_m denote Young's modulus of the bottom (as metal) and top e_c (as ceramic) surfaces of the FGM plate, respectively; e_m is Young's modulus of the homogeneous plate; and k is a parameter that indicates the material variation through the plate thickness. The material properties of a perfect FGM plate can be obtained when the volume fraction of porosity α is set to zero. Due to the small variations of the Poisson ratio v, it is assumed to be constant. Several forms of porosity have been studied in the present work (Wattanasakulpong 2014, Benferhat 2021a Tlidji *et al.* 2022, Kablia *et al.* 2023, Hassaine Daouadji *et al.* 2021c, Benferhat

Table 1 Deferent distribution forms of porosity

Distribution forms of Porosity
Uniform distribution shape of the porosity
$E_2 = (e_c - e_m)*((\frac{z}{t_2} + 0.5))^k + e_m - (e_c + e_m)*\frac{\alpha}{2}$ (2)
Form "X" distribution shape of the porosity
$E_2 = (e_c - e_m)*((\frac{z}{t_2} + 0.5))^k + e_m - (e_c + e_m)*\frac{\alpha}{2}*(2*\frac{z}{t_2})$ (3)
Form "O" distribution shape of the porosity
$E_2 = (e_c - e_m)*((\frac{z}{t_2} + 0.5))^k + e_m - (e_c + e_m)*\frac{\alpha}{2}*(1 - 2*\frac{\lvert z\rvert}{t_2})$ (4)
Inverted Form "V" distribution shape of the porosity
$E_2 = (e_c - e_m)*((\frac{z}{t_2} + 0.5))^k + e_m - (e_c + e_m)*\frac{\alpha}{2}*(\frac{1}{2} - \frac{z}{t_2})$ (5)
Form "V" distribution shape of the porosity
$E_2 = (e_c - e_m)*((\frac{z}{t_2} + 0.5))^k + e_m - (e_c + e_m)*\frac{\alpha}{2}*(\frac{1}{2} + \frac{z}{t_2})$ (6)

et al. 2021b, Rabahi *et al.* 2021d), such as “O”, “V” and X”, as follows (Table 1).

The linear constitutive relations of a FG plate can be written as

$$\begin{Bmatrix} \sigma_x \\ \sigma_y \\ \tau_{yz} \\ \tau_{xz} \\ \tau_{xy} \end{Bmatrix} = \begin{bmatrix} \frac{E(z)}{1-v^2} & \frac{vE(z)}{1-v^2} & 0 & 0 & 0 \\ \frac{vE(z)}{1-v^2} & \frac{E(z)}{1-v^2} & 0 & 0 & 0 \\ 0 & 0 & \frac{E(z)}{2(1-v)} & 0 & 0 \\ 0 & 0 & 0 & \frac{E(z)}{2(1-v)} & 0 \\ 0 & 0 & 0 & 0 & \frac{E(z)}{2(1-v)} \end{bmatrix} \begin{Bmatrix} \varepsilon_x \\ \varepsilon_y \\ \gamma_{yz} \\ \gamma_{xz} \\ \gamma_{xy} \end{Bmatrix} \tag{7}$$

where (σ_x, σ_y, τ_{xy}, τ_{yz}, τ_{xz}) and (ε_x, ε_y, γ_{xy}, γ_{yz}, γ_{xz}) are the stress and strain components, respectively, and A_{ij}, D_{ij} are the plate stiffness, defined by

Extensional matrix

$$A_{ij} = \int_{-h/2}^{h/2} Q_{ij} dz \tag{8a}$$

Flexural matrix

$$D_{ij} = \int_{-h/2}^{h/2} Q_{ij} z^2 dz \tag{8b}$$

where $A_{11}^{'}$, $D_{11}^{'}$ are defined as

$$A_{11}^{'} = \frac{A_{22}}{A_{11}A_{22}-A_{12}^2} \tag{9a}$$

$$D_{11}^{'} = \frac{D_{22}}{D_{11}D_{22}-D_{12}^2} \tag{9b}$$

2.3 Shear stress distribution along the imperfect FGM plate - concrete interface

The governing differential equation for the interfacial shear stress is expressed as (Benferhat 2021a)

$$\frac{d^2\tau(x)}{dx^2} - \frac{\left(A_{11}^{'}+\frac{b_2}{E_1A_1}+\frac{(y_1+t_2/2)(y_1+t_a+t_2/2)}{E_1I_1D_{11}^{'}+b_2}b_2D_{11}^{'}\right)}{\frac{t_a}{G_a}+\frac{t_1}{4G_1}}\tau(x) + \frac{\left(\frac{(y_1+t_2/2)}{E_1I_1D_{11}^{'}+b_2}D_{11}^{'}\right)}{\frac{t_a}{G_a}+\frac{t_1}{4G_1}}V_T(x) = 0 \tag{10}$$

For simplicity, the general solutions presented below are limited to loading which is either concentrated or uniformly distributed over part or the whole span of the beam, or both. For such loading, $d^2VT(x)/dx^2=0$, and the general solution to Eq. (10) is given by

$$\tau(x) = \Delta_1 \cosh(\varphi x) + \Delta_2 \sinh(\varphi x) + \frac{\left(\frac{y_1+\frac{t_2}{2}}{E_1I_1D_{11}^{'}+b_2}D_{11}^{'}\right)}{A_{11}{'}+\frac{b_2}{E_1A_1}+\frac{(y_1+t_2/2)(y_1+t_a+t_2/2)}{E_1I_1D_{11}^{'}+b_2}}V_T(x) \tag{11}$$

Where

$$\varphi = \sqrt{\frac{A_{11}^{'}+\frac{b_2}{E_1A_1}+\frac{(y_1+t_2/2)(y_1+t_a+t_2/2)}{E_1I_1D_{11}^{'}+b_2}b_2D_{11}^{'}}{\frac{t_a}{G_a}+\frac{t_1}{4G_1}}} \tag{12}$$

And Δ_1 and Δ_2 are constant coefficients determined from the boundary conditions. In the present study, a simply supported beam has been investigated which is subjected to a uniformly distributed load (Fig. 1). The interfacial shear stress for this uniformly distributed load at any point is written as (Benferhat 2021a)

$$\tau(x) = \left[\frac{\frac{K_1 y_1}{E_1 I_1} a}{2}(L-a) - \frac{\frac{1}{\frac{t_a}{G_a}+\frac{t_1}{4G_1}}}{\varphi^2}\left(\frac{y_1+\frac{t_2}{2}}{E_1 I_1 D_{11}^{'}+b_2} D_{11}^{'}\right)\right]\frac{q e^{-\varphi x}}{\varphi} + \frac{1}{\varphi^2\left(\frac{t_a}{G_a}+\frac{t_1}{4G_1}\right)}\left(\frac{y_1+\frac{t_2}{2}}{E_1 I_1 D_{11}^{'}+b_2} D_{11}^{'}\right) q\left(\frac{L}{2}-a-x\right) \quad 0 \le x \le L_P \tag{13}$$

Where q is the uniformly distributed load and x; a; L and L_p are defined in Fig. 1.

2.4 Normal stress distribution along the imperfect FGM plate - concrete interface

The following governing differential equation for the interfacial normal stress (Benferhat 2021a)

$$\frac{d^4\sigma_n(x)}{dx^4} + K_n\left(D_{11}^{'} + \frac{b_2}{E_1 I_1}\right)\sigma_n(x) - K_n\left(D_{11}^{'}\frac{t_2}{2} - \frac{y_1 b_2}{E_1 I_1}\right)\frac{d\tau(x)}{dx} + \frac{q K_n}{E_1 I_1} = 0 \tag{14}$$

The general solution to this fourth-order differential equation is

$$\sigma_n(x) = e^{-\psi x}[\Delta_3 \cos(\psi x) + \Delta_4 \sin(\psi x)] + e^{\psi x}[\Delta_5 \cos(\psi x) + \Delta_6 \sin(\psi x)] - \left(\frac{y_1 b_2 - \frac{D_{11}^{'} E_1 I_1 t_2}{2}}{D_{11}^{'} E_1 I_1 + b_2}\right)\frac{d\tau(x)}{dx} - \frac{1}{D_{11}^{'} E_1 I_1 + b_2} q \tag{15}$$

For large values of x it is assumed that the normal stress approaches zero and, as a result, $\Delta_5=\Delta_6=0$. The general solution therefore becomes

$$\sigma_n(x) = e^{-\psi x}[\Delta_3 \cos(\psi x) + \Delta_4 \sin(\psi x)] - \left(\frac{y_1 b_2 - \frac{D_{11}^{'} E_1 I_1 t_2}{2}}{D_{11}^{'} E_1 I_1 + b_2}\right)\frac{d\tau(x)}{dx} - \frac{1}{D_{11}^{'} E_1 I_1 + b_2} q \tag{16}$$

Where

$$\psi = \sqrt[4]{\frac{K_n}{4}\left(D_{11}^{'} + \frac{b_2}{E_1 I_1}\right)} \tag{17}$$

As is described by Benferhat (2021a), the constants Δ_3 and Δ_4 in Eq. (15) are determined using the appropriate boundary conditions and they are written as follows

$$\Delta_3 = \frac{K_n}{2\psi^3 E_1 I_1}[V_T(0) + \psi M_T(0)] - \frac{b_2 K_n\left(\frac{y_1}{E_1 I_1} - \frac{D_{11}^{'} t_2}{2 b_2}\right)}{2\psi^3}\tau(0) + \frac{\mu}{2\psi^3}\left(\frac{d^4\tau(0)}{dx^4} + \psi\frac{d^3\tau(0)}{dx^3}\right) \tag{18}$$

$$\Delta_4 = -\frac{K_n}{2\psi^2 E_1 I_1} M_T(0) - \frac{\mu}{2\psi^2}\frac{d^3\tau(0)}{dx^3} \tag{19}$$

$$\mu = \frac{y_1 b_2 - D_{11}^{'} E_1 I_1 t_2/2}{D_{11}^{'} E_1 I_1 + b_2} \tag{20}$$

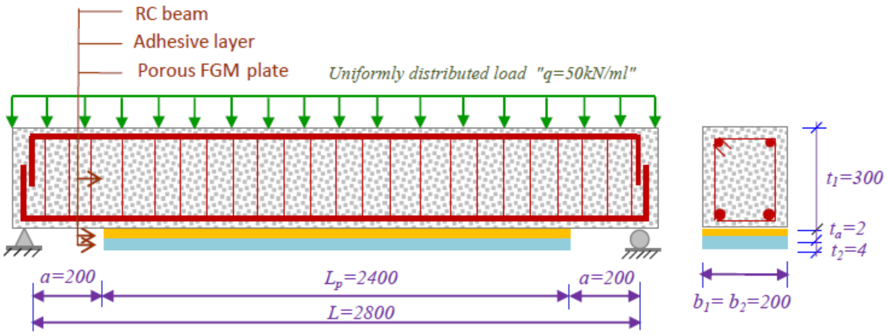

Fig. 2 Geometric characteristic of a RC beam reinforced by a perfect FGM plate

Table 2 Dimensions and material properties

Materials	E (GPa)	Width (mm)	Thickness (mm)
Concrete	30	b_1=200	t_1=300
Ceramic	380	b_2=200	t_2=4
Zirconia	151	b_2=200	t_2=4
Ti-6Al-4V	105.7	b_2=200	t_2=4
FGM	/	b_2=200	t_2=4
Metal (Al)	70	b_2=200	t_2=4
Adhesive	3	b_2=200	t_a=2

Table 3 Comparison of peak interfacial shear and normal stresses

	Theory		$\tau(x)$	$\sigma_n(x)$
RC beam with CFRP plate	Rabahi (2017)		1.874	0.996
	Tounsi (2009)		1.791	1.078
RC beam with GFRP plate	Rabahi (2017)		1.153	0.780
	Tounsi (2009)		1.085	0.826
RC beam with steel plate	Smith and Teng (2001)		4.443	2.247
	Tounsi (2009)		2.120	1.175
RC beam with Imperfect FGM plate	Present	α=0	1.5926	1.0192
		α=0.1	1.5050	0.98925
		α=0.2	1.5010	0.98765

The above expressions for the constants Δ_3 and Δ_4 has been left in terms of the bending moment $M_T(0)$ and shear force $V_T(0)$ at the end of the soffit plate. With the constants Δ_3 and Δ_4 determined, the interfacial normal stress can then be found using Eq. (15).

3. Numerical verification and discussions

In this section, numerical examples and parametric studies are presented for a simply supported

Table 4 Shear and normal stresses of a RC beam reinforced by a porous FGM plate

FGM plate	a	k=0		k=5		k=∞	
		$\tau(x)$	$\sigma_n(x)$	$\tau(x)$	$\sigma_n(x)$	$\tau(x)$	$\sigma_n(x)$
Al/Al_2O_3	a=0	2.7236	1.304	1.5926	1.0192	1.2979	0.91386
	a=0.1	2.6654	1.2956	1.5050	0.98925	1.0671	0.82071
	a=0.2	2.6036	1.2845	1.5010	0.98765	0.76555	0.68106
Al/ZrO_2	a=0	1.8738	1.1070	1.3375	0.92882	1.2979	0.91386
	a=0.1	1.8101	1.0880	1.2380	0.89076	1.1908	0.87192
	a=0.2	1.7428	1.0673	1.1300	0.84728	1.0718	0.82283
Ti-6Al-4V/Al_2O_3	a=0	2.5604	1.2760	1.6926	1.0516	1.5873	1.0171
	a=0.1	2.4946	1.2625	1.5605	1.0083	1.4238	0.96056
	a=0.2	2.4242	1.2471	1.4224	0.95997	1.2324	0.88851

Table 5 Shear and normal stresses of a RC beam reinforced by a porous FGM plate (Al/Al_2O_3) with different pore distribution

	Porosity distribution form	a=0.1		a=0.15		a=0.2	
		$\tau(x)$	$\sigma_n(x)$	$\tau(x)$	$\sigma_n(x)$	$\tau(x)$	$\sigma_n(x)$
FGM plate k=5	Uniform form	1.5050	0.98925	1.4857	0.98245	1.5010	0.98765
	'O' form	1.5680	1.0106	1.5916	1.0187	1.6574	1.0403
	'X' form	1.6089	1.0245	1.6296	1.0313	1.6686	1.0438
	'V' form	1.5580	1.0074	1.5600	1.0082	1.5878	1.0174
	'V' form reversed	1.6180	1.0273	1.6595	1.0410	1.7335	1.0644
FGM plate k=10	Uniform form	1.1178	0.84220	1.0144	0.79796	0.93526	0.76262
	'O' form	1.1913	0.87224	1.1532	0.85681	1.1667	0.86227
	'X' form	1.2749	0.90503	1.2457	0.89366	1.2203	0.88382
	'V' form	1.1992	0.87536	1.1365	0.84995	1.0876	0.82939
	'V' form reversed	1.2675	0.90238	1.2610	0.89977	1.2902	0.91090

FGM-plated concrete beam. The predicted stresses have been compared with those given in the literature. Then the mechanical and geometrical properties are varied in order to show their effect on the stress distribution along the externally of porous FGM plate-concrete interface (Fig. 2). For numerical applications, the mechanical and geometrical characteristics given in Table 2 are the same as those used by Tounsi (2009), Rabahi (2017) and Smith and Teng (2001).

Firstly, results of the present model of a concrete beam reinforced by a porous FGM plate were compared with those given by Tounsi (2009), Rabahi (2017) and Smith and Teng (2001) for a beam reinforced by CFRP, GFRP and steel plate in Table 3. It can be noted that the interfacial stresses are maximum when the RC beam is reinforced by a steel plate. Also, it is clear that the volume fraction of the porosity in reinforcement plate has a significant effect on shear and normal stress evolution.

Table 4 shows the interfacial stresses of a RC beam reinforced by a porous FGM plate. Several types of reinforcement plate are taken into account such as Al/Al_2O_3, Al/ZrO_2 and Ti-6Al-4V/Al_2O_3. The beams are considered subjected to a uniformly distributed load. The thickness of FGM plate is

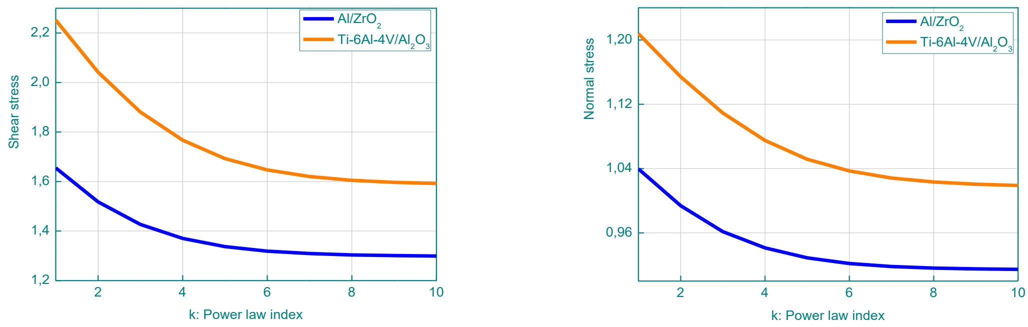

Fig. 3 Effect of the power law index on the shear and normal stress in RC beam reinforced by a perfect FGM plate

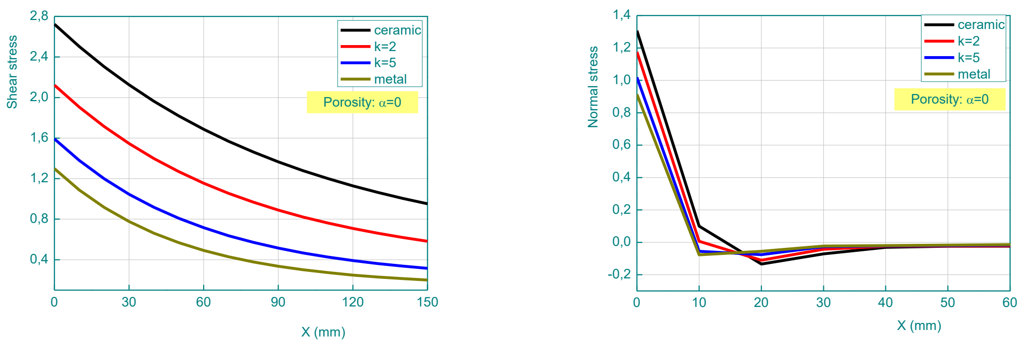

Fig. 4 Variation of the shear and normal stress versus the distance from the plate end in RC beam reinforced by a perfect FGM plate

taken to be (t_2=4 mm). It is observed that the shear and normal stresses diminishes with the increase of the volume fraction of the porosity and when the RC beam is reinforced by a Al/ZrO_2 plate. Table 5 presents the effect of distribution shape of the porosity in the interfacial stresses of RC beam reinforced by a porous FGM plate. Different distribution shape of porosity are taken into account namely: uniform, ‘O’, ‘X’, ‘V’ and ‘V’ inverted shape. The reinforcement FGM plate is in Al/Al_2O_3. It can be seen that the shear and normal stresses decrease for even distribution shape of porosity and increase for uneven distribution shape.

Figs. 3 and 4 show the variation of the interfacial stresses of RC beam strengthened with FGM plate versus the gradient index and the distance from the plate end, respectively. In Fig. 3 the reinforcement plate is made from Al/ZrO_2 and Ti-6Al-4V/Al_2O_3, and from Al/Al_2O_3 in Fig. 4. It can be seen that the shear and normal stress become highly when the reinforcement plate is made from Ti-6Al-4V/Al_2O_3. Also, these last become weaker when the power law index increase and when moving away from the end of the plate.

The variation of the interfacial stresses of RC beam strengthened with porous FGM plate versus the distance from the plate end and the power law index is shown in Figs. 5 and 6, respectively. The reinforcement plate is made from Al/Al_2O_3. The volume fraction of porosity varies from 0.1 to 0.2.

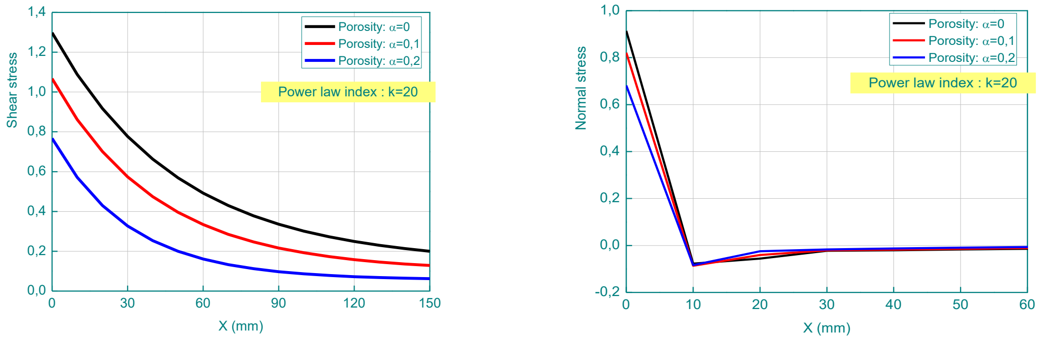

Fig. 5 Variation of the shear and normal stress versus the distance from the plate end in RC beam reinforced by porous FGM plate

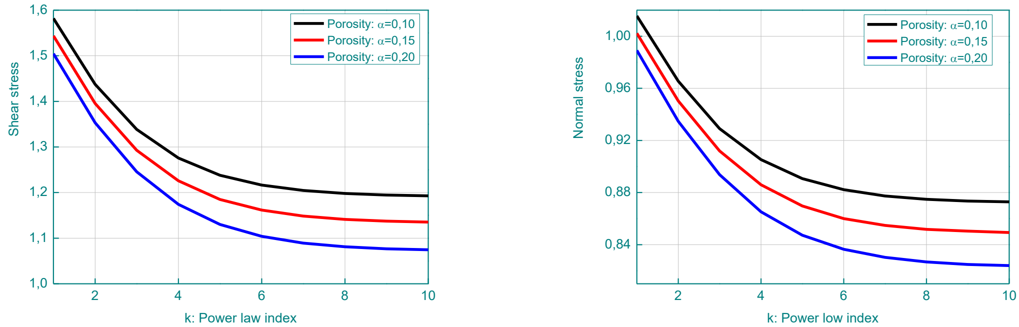

Fig. 6 Effect of the power index on the shear and normal stress in RC beam reinforced by a porous FGM plate

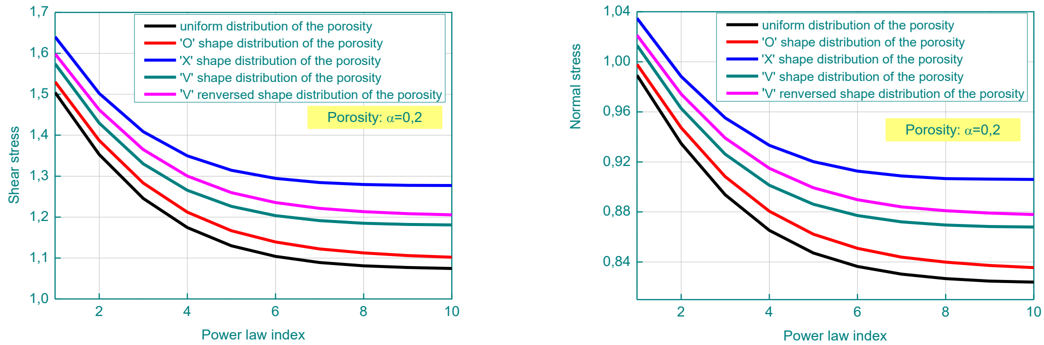

Fig. 7 Effect of distribution shape of porosity on the shear and normal stress in RC beam reinforced with a porous FGM plate

It can be seen that the interfacial stresses become weaker when the RC beam is reinforced by porous plates. In addition, it can be noticed that the volume fraction of porosity has more effect on the shear

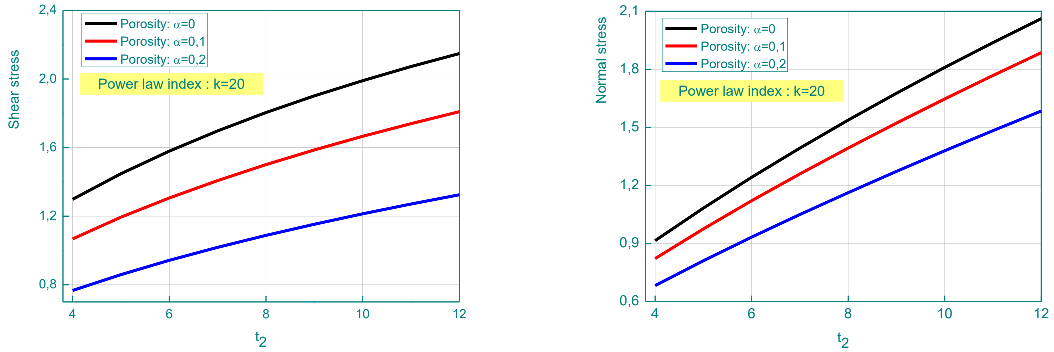

Fig. 8 Variation of the interfacial stress versus the distance from the plate end in RC beam reinforced with a porous FGM plate

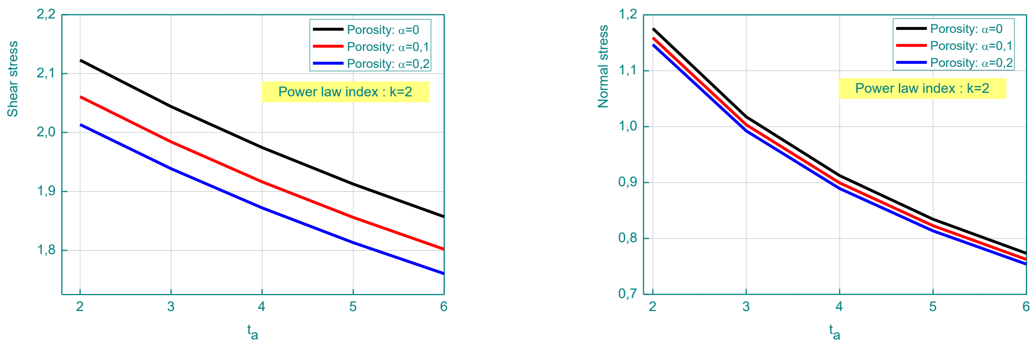

Fig. 9 Variation of the interfacial stress versus the distance from the plate end in RC beam reinforced with a porous FGM plate

and normal stress when the reinforcement plate becomes richer in metal (when k increase).

Fig. 7 presents the effect of distribution shape of porosity on the shear and normal stress in RC beam reinforced with a porous FGM plate. The reinforcement plate is made from Al/Al_2O_3. The volume fraction of porosity is taken to be α=0.2. Different distribution shape of porosity are taken into account namely: uniform, 'O', 'X', 'V' and 'V' inverted shape. It can be seen that the distribution shape of porosity has more effect on the interfacial stresses when the power law index increase. Also, it can be seen that the shear and normal stress become weaker for even distribution shape of porosity and highly for uneven distribution shape.

Figs. 8 and 9 depict the effect of the volume fraction of porosity on the interfacial stresses of RC beam strengthened with Al/Al_2O_3 FGM plate according to the thickness of plate and the adhesive layer, respectively. The gradient index is taken to be k=20 in Fig. 7 and I=2 in Fig. 9. The volume fraction of porosity varies from 0.1 to 0.2. From these figures, it can be concluded that the shear and normal stress increase with the increases of the thickness of reinforced plate and decrease with the increases of the thickness of the adhesive layer. As it was found in the previous figures, the interfacial stress decrease when the reinforcement plates containing porosity.

4. Conclusions

In the present research work, an original model is presented to predict the interfacial stresses of simply supported RC beam strengthened with porous FGM plate which is subjected to a uniformly distributed load. Both even distribution and uneven distribution of the porosity are taken into account in this study and the effective properties of reinforcement porous FGM plate are defined by theoretical formula with an additional term of porosity. According to the obtained results, it is found that the RC beams strengthened with porous FGM plate undergo weaker the interfacial stresses. Also, the results reveal that the shear and normal stress become weaker for even distribution shape of porosity and highly for uneven distribution shape. The impacts of the volume fraction of porosity, the power law index, the distribution shape of porosity, the mechanical and geometrical properties on the interfacial stresses along the externally of porous FGM plate-concrete interface are explored. With the studies presented and the results found the following conclusions can be taken, several of which may be useful recommendations for designers:

- The use of FGM materials as bending reinforcement provides increases in strength and rigidity for the reinforced concrete beam.
- There are stress concentrations at the end of the FGM plate. The normal stress concentration is a tensile stress but quickly towards to zero through a small oscillation. The initial delamination of the FGM plate from the reinforced concrete beam results from joints effects of the shear and normal stress at the end of the FGM plate.
- The maximum edge interfacial stresses increase with increasing the stiffness of the plate (as a function of k - power law index, and as a function of the percentage of the porosity of the imperfect FGM material).
- The interfacial stresses are influenced by the geometry parameters such as thickness of the adhesive layer and FGM plate in range of the different degrees. It is shown that the edge stresses and levels increase obviously with the increase of the thickness of the FGM plate. However, it is seen that increasing the thickness of the adhesive layer leads to significant reduction in the peak interfacial stresses.
- Another outcome based on the parametric study indicates that extending the imperfect FGM strip as close as possible to the support reduces the stresses at the edge.
- Several factors are involved in the mechanical behaviour of the reinforced concrete beams that need to be taken into account when evaluating the use of imperfect FGM materials in external reinforcement. The analysis of the structural behaviour is more complex than the other bending elements reinforced.

In perspective, it is desirable to take into account:

- Effect of boundary conditions gives more clarification on FGM-RC hybrid beam
- Also take into account the effect of prestressing on the imperfect FGM plates
- A numerical analysis by finite element will be very interesting
- Temperature effect on FGM-RC hybrid beam
- The effect of the hygrethermal conditions of the FGM plates
- Applications on FGM-RC hybrid hyperstatic beam

Acknowledgments

This research was supported by the Algerian Ministry of Higher Education and Scientific

Research (MESRS) as part of the grant for the PRFU research project n° A01L02UN140120200002 and by the University of Tiaret, in Algeria.

References

Abderezak, R., Daouadji, T.H. and Rabia, B. (2021a), "Modeling and analysis of the imperfect FGM-damaged RC hybrid beams", *Adv. Comput. Des.*, **6**(2), 117-133. http://doi.org/10.12989/acd.2021.6.2.117.

Abderezak, R., Daouadji, T.H. and Rabia, B. (2021b), "Aluminum beam reinforced by externally bonded composite materials", *Adv. Mater. Res.*, **10**(1), 23-44. http://doi.org/10.12989/amr.2021.10.1.023.

Abderezak, R., Daouadji, T.H. and Rabia, B. (2021c), "Fiber reinforced polymer in civil engineering: Shear lag effect on damaged RC cantilever beams bonded by prestressed plate", *Coupled Syst. Mech.*, **10**(4), 299-316. http://doi.org/10.12989/csm.2021.10.4.299.

Abderezak, R., Daouadji, T.H. and Rabia, B. (2021d), "New solution for damaged porous RC cantilever beamsstrengthening by composite plate", *Adv. Mater. Res.*, **10**(3), 169-194. http://doi.org/10.12989/amr.2021.10.3.169.

Abderezak, R., Daouadji, T.H. and Rabia, B. (2022b), "Analysis and modeling of hyperstatic RC beam bonded by composite plate symmetrically loaded and supported", *Steel Compos. Struct.*, **45**(4), 591-603. https://doi.org/10.12989/scs.2022.45.4.591.

Abderezak, R., Daouadji, T.H. and Tayeb, B. (2023), "Composite aluminum-slab RC beam bonded by a prestressed hybrid carbon-glass composite material", *Struct. Eng. Mech.*, **85**(5), 573-592. https://doi.org/10.12989/sem.2023.85.5.573.

Abderezak, R., Daouadji, T.H., Abbes, B., Rabia, B., Belkacem, A. and Abbes, F. (2017), "Elastic analysis of interfacial stress concentrations in CFRP-RC hybrid beams: Effect of creep and shrinkage", *Adv. Mater. Res.*, **6**(3), 257-278. http://doi.org/10.12989/amr.2017.6.3.257.

Abderezak, R., Rabia, B. and Daouadji, T.H. (2022a), "Rehabilitation of RC structural elements: Application for continuous beams bonded by composite plate under a prestressing force", *Adv. Mater. Res.*, **11**(2), 91-109. https://doi.org/10.12989/amr.2022.11.2.091.

Adim, B. and Daouadji, T.H. (2016b), "Effects of thickness stretching in FGM plates using a quasi-3D higher order shear deformation theory", *Adv. Mater. Res.*, **5**(4), 223-244. https://doi.org/10.12989/amr.2016.5.4.223.

Adim, B., Daouadji, T.H. and Abbes, B. (2016), "Buckling analysis of anti-symmetric cross-ply laminated composite plates under different boundary conditions", *Int. Appl. Mech.*, **52**(6), 126-141. https://doi.org/10.1007/s10778-016-0787-x.

Adim, B., Daouadji, T.H., Rabia, B. and Hadji, L. (2016a), "An efficient and simple higher order shear deformation theory for bending analysis of composite plates under various boundary conditions", *Earthq. Struct.*, **11**(1), 63-82. https://doi.org/10.12989/eas.2016.11.1.063.

Ahmed, R.A., Al-Maliki, A.F. and Faleh, N.M. (2020), "Dynamic characteristics of multi-phase crystalline porous shells with using strain gradient elasticity", *Adv. Nano Res.*, **8**(2), 157-167. https://doi.org/10.12989/anr.2020.8.2.157.

Aicha, K., Rabia, B., Daouadji, T.H. and Bouzidene, A. (2020), "Effect of porosity distribution rate for bending analysis of imperfect FGM plates resting on Winkler-Pasternak foundations under various boundary conditions", *Coupled Syst. Mech.*, **9**(6), 575-597. http://doi.org/10.12989/csm.2020.9.6.575.

Bekkaye, T.H.L., Fahsi, B., Bousahla, A.A., Bourada, F., Tounsi, A., Benrahou, K.H. and Al-Zahrani, M.M. (2020), "Porosity-dependent mechanical behaviors of FG plate using refined trigonometric shear deformation theory", *Comput. Concrete*, **26**(5), 439-450. http://doi.org/10.12989/cac.2020.26.5.439.

Benferhat Rabia, Hassaine Daouadji Tahar and Rabahi Abderezak (2021c) "Effect of porosity on fundamental frequencies of FGM sandwich plates", *Compos. Mater. Eng.*, **3**(1), 25-40. http://doi.org/10.12989/cme.2021.3.1.025.

Benferhat, R., Daouadji, T.H. and Mansour, M.S. (2016), "Free vibration analysis of FG plates resting on the elastic foundation and based on the neutral surface concept using higher order shear deformation theory", Comptes Rendus Mecanique, **344**(9), 631-641. https://doi.org/10.1016/j.crme.2016.03.002.

Benferhat, R., Hassaine Daouadji, T. and Rabahi, A. (2021b), "Analysis and sizing of RC beams reinforced by external bonding of imperfect functionally graded plate", *Adv. Mater. Res.*, **10**(2), 77-98. http://doi.org/10.12989/amr.2021.10.2.077.

Bensattalah, T., Zidour, M. and Hassaine Daouadji, T. (2018), "Analytical analysis for the forced vibration of CNT surrounding elastic medium including thermal effect using nonlocal Euler-Bernoulli theory", *Adv. Mater. Res.*, **7**(3), 163-174. https://doi.org/10.12989/amr.2018.7.3.163.

Bourada, F., Bousahla, A.A., Tounsi, A., Bedia, E.A., Mahmoud, S.R., Benrahou, K.H. and Tounsi, A. (2020), "Stability and dynamic analyses of SW-CNT reinforced concrete beam resting on elastic-foundation", *Comput. Concrete*, **25**(6), 485-495. http://doi.org/10.12989/cac.2020.25.6.485.

Daouadji, T.H. (2013), "Analytical analysis of the interfacial stress in damaged reinforced concrete beams strengthened by bonded composite plates", *Strength Mater.*, **45**(5), 587-597. https://doi.org/10.1007/s11223-013-9496-4.

Daouadji, T.H. (2017), "Analytical and numerical modeling of interfacial stresses in beams bonded with a thin plate", *Adv. Comput. Des.*, **2**(1), 57-69. https://doi.org/10.12989/acd.2017.2.1.057.

Daouadji, T.H., Abderezak, R. and Rabia, B. (2022), "New technique for repairing circular steel beams by FRP plate", *Adv. Mater. Res.*, **11**(3), 171-190. https://doi.org/10.12989/amr.2022.11.3.171.

Daouadji, T.H., Chedad, A. and Adim, B. (2016b), "Interfacial stresses in RC beam bonded with a functionally graded material plate", *Struct. Eng. Mech.*, **60**(4), 693-705. http://doi.org/10.12989/sem.2016.60.4.693.

Daouadji, T.H., Rabahi, A., Abbes, B. and Adim, B. (2016a), "Theoretical and finite element studies of interfacial stresses in reinforced concrete beams strengthened by externally FRP laminates plate", *J. Adhes. Sci. Technol.*, **30**(12), 1253-1280. https://doi.org/10.1080/01694243.2016.1140703.

Ebrahimi, F. and Seyfi, A. (2022), "Studying propagation of wave in metal foam cylindrical shells with graded porosities resting on variable elastic substrate", *Eng. Comput.*, **38**, 379-395. https://doi.org/10.1007/s00366-020-01069-w.

Ebrahimi, F., Jafari, A. and Selvamani, R. (2020), "Thermal buckling analysis of magneto-electro-elastic porous FG beam in thermal environment", *Adv. Nano Res.*, **8**(1), 83-94. https://doi.org/10.12989/anr.2020.8.1.083.

Fenjan, R.M., Faleh, N.M. and Ridha, A.A. (2020), "Strain gradient based static stability analysis of composite crystalline shell structures having porosities", *Steel Compos. Struct.*, **36**(6), 631-642. https://doi.org/10.12989/scs.2020.36.6.631.

Guenaneche, B., Benyoucef, S., Tounsi, A. and Adda Bedia, E.A. (2019), "Improved analytical method for adhesive stresses in plated beam: Effect of shear deformation", *Adv. Concrete Constr.*, **7**(3), 151-166. http://doi.org/10.12989/acc.2019.7.3.151.

Ishihara, M., Yoshida, T., Ootao, Y. and Kameo, Y. (2020), "Hygrothermoelasticity in a porous cylinder under nonlinear coupling between heat and moisture", *Struct. Eng. Mech.*, **75**(1), 59-69. https://doi.org/10.12989/sem.2020.75.1.059.

Jena, S.K., Chakraverty, S. and Malikan, M. (2021), "Application of shifted Chebyshev polynomial-based Rayleigh-Ritz method and Navier's technique for vibration analysis of a functionally graded porous beam embedded in Kerr foundation", *Eng. Comput.*, **37**, 3569-3589. https://doi.org/10.1007/s00366-020-01018-7.

Kablia, A., Benferhat, R. and Daouadji, T.H. (20022), "Dynamic of behavior for imperfect FGM plates resting on elastic foundation containing various distribution rates of porosity: Analysis and modeling", *Coupled Syst. Mech.*, **11**(5), 389-409. https://doi.org/10.12989/csm.2022.11.5.389.

Kablia, A., Benferhat, R., Daouadji, T.H. and Abderezak, R. (2023), "Free vibration of various types of FGP sandwich plates with variation in porosity distribution", *Struct. Eng. Mech.*, **85**(1), 1-14. https://doi.org/10.12989/sem.2023.85.1.001.

Kaddari, M., Kaci, A., Bousahla, A.A., Tounsi, A., Bourada, F., Bedia, E.A. and Al-Osta, M.A. (2020), "A study on the structural behaviour of functionally graded porous plates on elastic foundation using a new quasi-3D model: Bending and free vibration analysis", *Comput. Concrete*, **25**(1), 37-57.

http://doi.org/10.12989/cac.2020.25.1.037.
Karami, B., Shahsavari, D., Janghorban, M. and Li, L. (2020), "Free vibration analysis of FG nanoplate with poriferous imperfection in hygrothermal environment", *Struct. Eng. Mech.*, **73**(2), 191-207. https://doi.org/10.12989/sem.2020.73.2.191.
Khaniki, H.B., Ghayesh, M.H., Hussain, S. and Amabili, M. (2022), "Porosity, mass and geometric imperfection sensitivity in coupled vibration characteristics of CNT-strengthened beams with different boundary conditions", *Eng. Comput.*, **38**, 2313-2339. https://doi.org/10.1007/s00366-020-01208-3.
Khazaei, P. and Mohammadimehr, M. (2020), "Size dependent effect on deflection and buckling analyses of porous nanocomposite plate based on nonlocal strain gradient theory", *Struct. Eng. Mech.*, **76**(1), 27-56. https://doi.org/10.12989/sem.2020.76.1.027.
Laib, S., Meftah, S.A., Youzera, H., Ziane, N. and Tounsi, A. (2021), "Vibration and damping characteristics of the masonry wall strengthened with bonded fibre composite patch with viscoelastic adhesive layer", *Comput. Concrete*, **27**(3), 253-268. http://doi.org/10.12989/cac.2021.27.3.253.
Mirjavadi, S.S., Forsat, M., Barati, M.R. and Hamouda, A.M.S. (2020a), "Post-buckling of higher-order stiffened metal foam curved shells with porosity distributions and geometrical imperfection", *Steel Compos. Struct.*, **35**(4), 567-578. https://doi.org/10.12989/scs.2020.35.4.567.
Mirjavadi, S.S., Forsat, M., Nia, A.F., Badnava, S. and Hamouda, A.M.S. (2020b), "Nonlocal strain gradient effects on forced vibrations of porous FG cylindrical nanoshells", *Adv. Nano Res.*, **8**(2), 149-156. https://doi.org/10.12989/anr.2020.8.2.149.
Mohammadimehr, M. and Meskini, M. (2020), "Analysis of porous micro sandwich plate: Free and forced vibration under magneto-electro-elastic loadings", *Adv. Nano Res.*, **8**(1), 69-82. https://doi.org/10.12989/anr.2020.8.1.069.
Rabia, B., Abderezak, R., Daouadji, T.H., Abbes, B., Belkacem, A. and Abbes, F. (2018), "Analytical analysis of the interfacial shear stress in RC beams strengthened with prestressed exponentially-varying properties plate", *Adv. Mater. Res.*, **7**(1), 29-44. https://doi.org/10.12989/amr.2018.7.1.029.
Rabia, B., Daouadji, T.H. and Abderezak, R. (2019), "Effect of distribution shape of the porosity on the interfacial stresses of the FGM beam strengthened with FRP plate", *Earthq. Struct.*, **16**(5), 601-609. https://doi.org/10.12989/eas.2019.16.5.601.
Rabia, B., Daouadji, T.H. and Abderezak, R. (2019), "Effect of porosity in interfacial stress analysis of perfect FGM beams reinforced with a porous functionally graded materials plate", *Struct. Eng. Mech.*, **72**(3), 293-304. https://doi.org/10.12989/sem.2019.72.3.293.
Rabia, B., Daouadji, T.H. and Abderezak, R. (2020), "Predictions of the maximum plate end stresses of imperfect FRP strengthened RC beams: Study and analysis", *Adv. Mater. Res.*, **9**(4), 265-287. http://doi.org/10.12989/amr.2020.9.4.265.
Rabia, B., Daouadji, T.H. and Abderezak, R. (2021a), "Effect of air bubbles in concrete on the mechanical behavior of RC beams strengthened in flexion by externally bonded FRP plates under uniformly distributed loading", *Compos. Mater. Eng.*, **3**(1), 41-55. http://doi.org/ 10.12989/cme.2021.3.1.041.
Rabia, B., Tahar, H.D. and Abderezak, R. (2020), "Thermo-mechanical behavior of porous FG plate resting on the Winkler-Pasternak foundation", *Coupled Syst. Mech.*, **9**(6), 499-519. http://doi.org/10.12989/csm.2020.9.6.499.
Rostami, R. and Mohammadimehr, M. (2022), "Vibration control of rotating sandwich cylindrical shell-reinforced nanocomposite face sheet and porous core integrated with functionally graded magneto-electro-elastic layers", *Eng. Comput.*, **38**, 87-100. https://doi.org/10.1007/s00366-020-01052-5.
Sadoughifar, A., Farhatnia, F., Izadinia, M. and Talaeetaba, S. B. (2020), "Size-dependent buckling behaviour of FG annular/circular thick nanoplates with porosities resting on Kerr foundation based on new hyperbolic shear deformation theory", *Struct. Eng. Mech.*, **73**(3), 225-238. https://doi.org/10.12989/sem.2020.73.3.225.
Safaei, B. (2020), "The effect of embedding a porous core on the free vibration behavior of laminated composite plates", *Steel Compos. Struct.*, **35**(5), 659-670. https://doi.org/10.12989/scs.2020.35.5.659.
Safeer, M., Khadimallah, M.A., Taj, M., Hussain, M., Elaloui, E. and Tounsi, A. (2021), "Strength performance with buckling analysis of Intermediate filaments by consideration nonlocal parameters", *Comput. Concrete*,

28(1), 69-75. http://doi.org/10.12989/cac.2021.28.1.069.

Sahmani, S., Fattahi, A.M. and Ahmed, N.A. (2020), "Analytical treatment on the nonlocal strain gradient vibrational response of postbuckled functionally graded porous micro-/nanoplates reinforced with GPL", *Eng. Comput.*, **36**, 1559-1578. https://doi.org/10.1007/s00366-019-00782-5.

She, G.L., Liu, H.B. and Karami, B. (2020), "On resonance behavior of porous FG curved nanobeams", *Steel Compos. Struct.*, **36**(2), 179-186. https://doi.org/10.12989/scs.2020.36.2.179.

Shen, H.S., Teng, J.G. and Yang, J. (2001), "Interfacial stresses in beams and slabs bonded with thin plate", *J. Eng. Mech.*, **127**(4), 399-406. https://doi.org/10.1061/(ASCE)0733-9399(2001)127:4(399).

Si, H., Shen, D., Xia, J. and Tahouneh, V. (2020), "Vibration behavior of functionally graded sandwich beam with porous core and nanocomposite layers", *Steel Compos. Struct.*, **36**(1), 1-16. https://doi.org/10.12989/scs.2020.36.1.001.

Smith, S.T. and Teng, J.G. (2001), "Interfacial stresses in plated beams", *Eng. Struct.*, **23**(7), 857-871. https://doi.org/10.1016/S0141-0296(00)00090-0.

Tahar, H.D., Abderezak, R. and Rabia, B. (2021d), "A new model for adhesive shear stress in damaged RC cantilever beam strengthened by composite plate taking into account the effect of creep and shrinkage", *Struct. Eng. Mech.*, **79**(5), 531-540. http://doi.org/10.12989/sem.2021.79.5.531.

Tahar, H.D., Abderezak, R. and Rabia, B. (2021e), "Hyperstatic steel structure strengthened with prestressed carbon/glass hybrid laminated plate", *Coupled Syst. Mech.*, **10**(5), 393-414. https://doi.org/10.12989/csm.2021.10.5.393.

Tahar, H.D., Abderezak, R., Rabia, B. and Tounsi, A. (2021b), "Performance of damaged RC continuous beams strengthened by prestressed laminates plate: Impact of mechanical and thermal properties on interfacial stresses", *Coupled Syst. Mech.*, **10**(2), 161-184. http://doi.org/10.12989/csm.2021.10.2.161.

Tahar, H.D., Abderezak, R., Rabia, B. and Tounsi, A. (2021c), "Impact of thermal effects in FRP-RC hybrid cantilever beams", *Struct. Eng. Mech.*, **78**(5), 573-583. http://doi.org/10.12989/sem.2021.78.5.573.

Tahar, H.D., Boussad, A., Abderezak, R., Rabia, B., Fazilay, A. and Belkacem, A. (2019), "Flexural behaviour of steel beams reinforced by carbon fiber reinforced polymer: Experimental and numerical study", *Struct. Eng. Mech.*, **72**(4), 409-419. https://doi.org/10.12989/sem.2019.72.4.409.

Tahar, H.D., Tayeb, B., Abderezak, R. and Tounsi, A. (2021a), "New approach of composite wooden beam-reinforced concrete slab strengthened by external bonding of prestressed composite plate: Analysis and modeling", *Struct. Eng. Mech.*, **78**(3), 319-332. http://doi.org/10.12989/sem.2021.78.3.31.

Taj, M., Khadimallah, M.A., Hussain, M., Fareed, K., Safeer, M., Khedher, K.M. and Tounsi, A. (2021), "Thermal stress effects on microtubules based on orthotropic model: Vibrational analysis", *Adv. Concrete Constr.*, **11**(3), 255-260. http://doi.org/10.12989/acc.2021.11.3.255.

Tayeb, B. and Daouadji, T.H. (2020), "Improved analytical solution for slip and interfacial stress in composite steel-concrete beam bonded with an adhesive", *Adv. Mater. Res.*, **9**(2), 133-153. https://doi.org/10.12989/amr.2020.9.2.133.

Tayeb, B., Daouadji, T.H., Abderezak, R. and Tounsi, A. (2021), "Structural bonding for civil engineering structures: New model of composite I-steel-concrete beam strengthened with CFRP plate", *Steel Compos. Struct.*, **41**(3), 417-435. https://doi.org/10.12989/scs.2021.41.3.417.

Thanh, C.L., Nguyen, T.N., Vu, T.H., Khatir, S. and Abdel Wahab, M. (2022), "A geometrically nonlinear size-dependent hypothesis for porous functionally graded micro-plate", *Eng. Comput.*, **38**, 449-460. https://doi.org/10.1007/s00366-020-01154-0.

Tlidji, Y., Benferhat, R. and Tahar, H.D. (2021a), "Study and analysis of the free vibration for FGM microbeam containing various distribution shape of porosity", *Struct. Eng. Mech.*, **77**(2), 217-229. http://doi.org/10.12989/sem.2021.77.2.217.

Tlidji, Y., Benferhat, R., Daouadji, T.H., Tounsi, A. and Trinh, L.C. (2022), "Free vibration analysis of FGP nanobeams with classical and non-classical boundary conditions using State-space approach", *Adv. Nano Res.*, **13**(5), 453-463. https://doi.org/10.12989/anr.2022.13.5.453.

Tlidji, Y., Benferhat, R., Trinh, L.C., Tahar, H.D. and Abdelouahed, T. (2021b), "New state-space approach to dynamic analysis of porous FG beam under different boundary conditions", *Adv. Nano Res.*, **11**(4), 347-359. https://doi.org/10.12989/anr.2021.11.4.347.

Tounsi, A., Daouadji, T.H. and Benyoucef, S. (2009), “Interfacial stresses in FRP-plated RC beams: Effect of adherend shear deformations”, *Int. J. Adhes. Adhes.*, **29**, 313-351. https://doi.org/10.1016/j.ijadhadh.2008.06.008.

Wattanasakulpong, N. and Ungbhakorn, V. (2014), “Linear and nonlinear vibration analysis of elastically restrained ends FGM beams with porosities”, *Aerosp. Sci. Technol.*, **32**(1), 111-120. https://doi.org/10.1016/j.ast.2013.12.002.

Yu, B., Ding, Z., Liu, S. and Li, B. (2021), “Theoretical and practical models for shear strength of corroded reinforced concrete columns”, *Struct. Eng. Mech.*, **79**(5), 565-578. http://doi.org/10.12989/sem.2021.79.5.565.

Yüksel, Y.Z. and Akbaş, Ş.D. (2021), “Hygrothermal stress analysis of laminated composite porous plates”, *Struct. Eng. Mech.*, **80**(1), 1-13. http://doi.org/10.12989/sem.2021.80.1.001.

Zhou, C., Zhan, Z., Zhang, J., Fang, Y. and Tahouneh, V. (2020), “Vibration analysis of FG porous rectangular plates reinforced by graphene platelets”, *Steel Compos. Struct.*, **34**(2), 215-226. https://doi.org/10.12989/scs.2020.34.2.215.

Zohra, A., Benferhat, R., Tahar, H.D. and Tounsi, A. (2021), “Analysis on the buckling of imperfect functionally graded sandwich plates using new modified power-law formulations”, *Struct. Eng. Mech.*, 77(6), 797-807. http://doi.org/10.12989/sem.2021.77.6.797.

CC